Conformal growth of *Arabidopsis* leaves.

Graeme Mitchison[1,*],

1 Sainsbury Laboratory, Cambridge University, Cambridge, UK

*** gjm12@cam.ac.uk**

Abstract

I show that Arabidopsis leaf growth can be described with high accuracy by a conformal map, where expansion is locally isotropic (the same in all directions) but the amount of expansion can vary with position. Data obtained by tracking leaf growth over time can be reproduced with almost 90% accuracy by such a map. At 7-8 days, 67% of leaf growth is accounted for by uniform expansion of the whole leaf, but the best fitting conformal map, having 89% accuracy, is achieved by adding nonlinear terms to this linear map. Growth according to a conformal map has the property of maintaining the flatness of a leaf. To understand how such a map is generated, one can mathematically subtract the effects of tissue expansion and calculate the underlying distribution of growth rate. This turns out to be a simple linear gradient, which could be generated by a diffusible signal.

Introduction

Increasingly precise information about plant growth is becoming available, and in particular the growth pattern of developing leaves and petals has been mapped in some detail [1, 2, 3, 4, 5, 6, 7, 8]. These growth patterns have been accounted for by models in which growth regulators operate within specified regions of the leaf [7], polarity fields control the predominant direction of growth [8], and gene networks regulate the succession of morphogenetic events in a combinatorial fashion [4, 5, 8].

A different type of explanation, with its roots in physics and engineering, goes back to D'Arcy Thompson and his famous book, On Growth and Form [9]. Thompson discusses leaf growth in terms of transformations extending over the whole leaf area, and points to possible underlying physical mechanisms. In a footnote ([9], p 1084), he draws attention to the resemblance of certain mappings to conformal transformations. These are transformations of the plane that preserve angles locally, and are generated by isotropic local expansion. The amount of expansion can vary with position, but at any point expansion occurs to the same extent in all directions. Conformal maps are very important in physics and engineering, because they are intimately connected with diffusion, hydrodynamics and electrical fields. There is also a close connection with complex analytic functions, which are maps from the complex plane to itself (the

complex plane, or Argand diagram, represents complex numbers $x + iy$). Every complex analytic function is conformal and vice-versa.

A recent revival of this approach by Jones and Mahadevan [10] looks at the larger class of quasi-conformal mappings (where the expansion is not necessarily isotropic) and shows how to use them for various kinds of morphometry. Another contribution comes from Wolfram, in a footnote in his magnum opus A New Kind of Science [11], where he proposes that leaf growth might follow a conformal mapping, and that this would preserve the flatness of the leaf surface. He also observes that conformal mappings might be generated biologically by a diffusion-based mechanism, since the components of these mappings satisfy the equilibrium diffusion equation.

In a certain sense, Wolfram's assertion about flatness is a tautology, since a conformal map is planar and a planar map will preserve flatness. The real content lies in the proposal that leaf growth is locally isotropic. If this is true, then to be planar amounts to being conformal. At first sight, it seems unlikely that leaf growth is locally isotropic; for instance, clones become markedly elongated in petals (Figure 2 in [8]) and leaves (Figure 2 in [7]).

The surprise is that Wolfram's assumption turns out to be largely correct. I show here that, using data kindly made available by Professor Rolland-Lagan, that the growth of *Arabidopsis* leaves approximates remarkably well to a conformal mapping, about 90% of the growth being accounted for by such a map. This suggests, as Wolfram notes, an underlying diffusion-based mechanism. A fascinating question is then raised by the relationship between this kind of explanation and the gene-based interpretation discussed initially.

Results

The data used here consist of a set of observations of individual *Arabidopsis* leaves, each of which has a number of beads attached to its surface that are tracked day by day. The earliest time point is day 7 after sowing, and there are altogether thirteen leaves that were tracked till day 12. As we shall see, the earliest time step, day 7 to day 8, provides the most interesting data, since uniform expansion, with a constant relative growth rate (RGR) over the entire leaf, increasingly takes over with increasing age. Figure 1 shows the displacement of beads between days 7 and 8 for several leaves.

Figure 1: *The displacement of beads between day 7 and day 8 for four leaves, the one with the greatest number of beads (leaf 1) and three others. The green outline is the margin of the leaf at day 7 and the blue outline that at day 8. The beads are shown as small circles at the start of the arrow, which ends at the position of that bead at day 8. The axes show the size of the leaves in microns. Note that the origin of the x- and y-coordinates lies at the approximate centre of the leaves.*

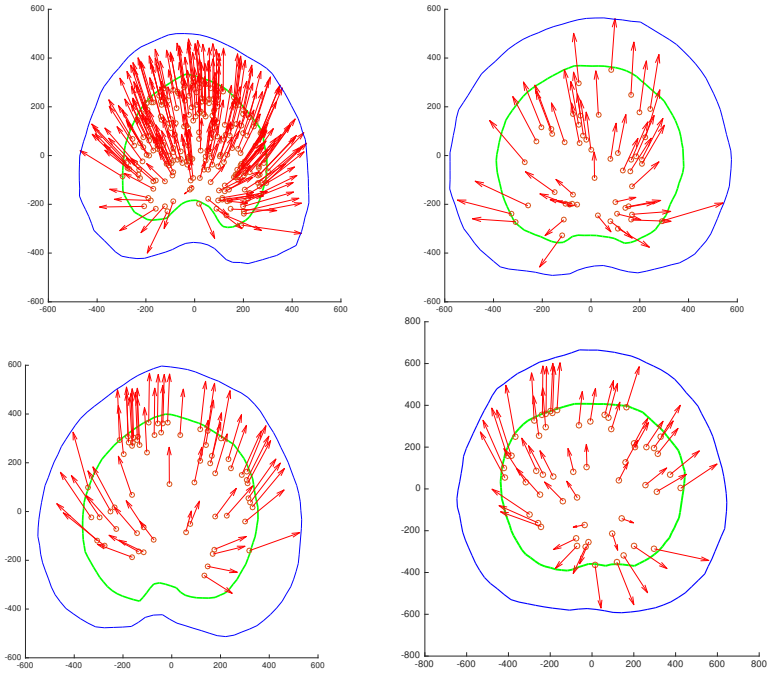

Fitting a conformal map to growth

The *Arabidopsis* leaves being studied are reasonably flat, as shown in Figure 3 of [3], and so it is a good approximation to describe their growth as a map from the plane into itself. As remarked earlier, conformal maps can be interpreted as functions from the complex plane to itself. In the complex plane, the point (x, y) represents a complex number $x + iy$. Thus the strategy used here is to try to approximate the movement of a bead from a point (x, y) to a point (u, v) by a complex function $f(x + iy) = u + iv$.

A very simple example of such a function is the linear function $f(z) = a+bz$, where $z = x + iy$, and $a = a_0 + ia_1$ and $b = b_0 + ib_1$ are complex constants. This map takes the point (x, y) to (u, v), where $u = a_0 + b_0x - b_1y$ and $v = a_1 + b_0y + b_1x$. This amounts to a shift of origin to the point a in the complex plane, a rotation by $\arg b = \arctan(b_1/b_0)$, and a constant RGR everywhere on the leaf of $|b| = \sqrt{b_0^2 + b_1^2}$.

Thus a linear complex map can capture the relative positioning and orientation of the leaf between successive days, which have to do with the experimental

set-up; it can also account for a constant RGR, which is a parameter with biological significance. The best-fitting linear complex map, found by least squares fitting of the bead data points, therefore gives us an estimate of both the experimental parameters and the intrinsic uniform isotropic growth. The difference between the final bead position predicted by this linear model and the true position, i.e. the linear model *residual*, indicates what else is going on.

The size of the residual can be measured by summing the lengths of the residual vectors and dividing this by the sum of the total bead displacement observed experimentally. This *normalised residual* has an average value over all the leaves of 0.33; see Figure 2 and Table 3. Equivalently, one can say that 67% of the displacement is accounted for by a linear model.

Figure 2: *Histogram showing the normalised residuals for linear, quadratic and cubic complex polynomials. The normalised residual is defined as* $\sum_i |v_i - l_i| / \sum_i |v_i|$*, where* v_i *is the vector between bead positions on successive days,* l_i *is the residual vector, and* i *runs over all beads. The x-axis list the leaves according to the numbering used here; see Table 2.*

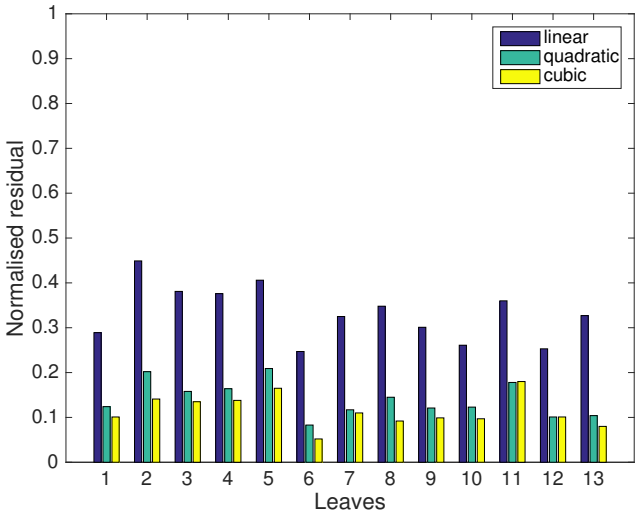

We now turn to the distribution on the leaf lamina of the residual from a linear model, shown in Figure 3. This is very striking: as one follows a path round the perimeter of the leaf, the residual vectors rotate *twice as fast* as the radial vector. This is what is expected of a quadratic complex function, as shown in Figure 4. Note that the origin of the leaf's coordinate system is in the approximate centre of the leaf, and that of the complex quadratic lies at the centre of the circle.

Figure 3: *The residual movement of beads after subtracting the best-fitting linear map, for four leaves and the time period 7-8 days. Note the rotation of the arrows at twice the speed of the radius, and compare with the quadratic function in Figure 4*

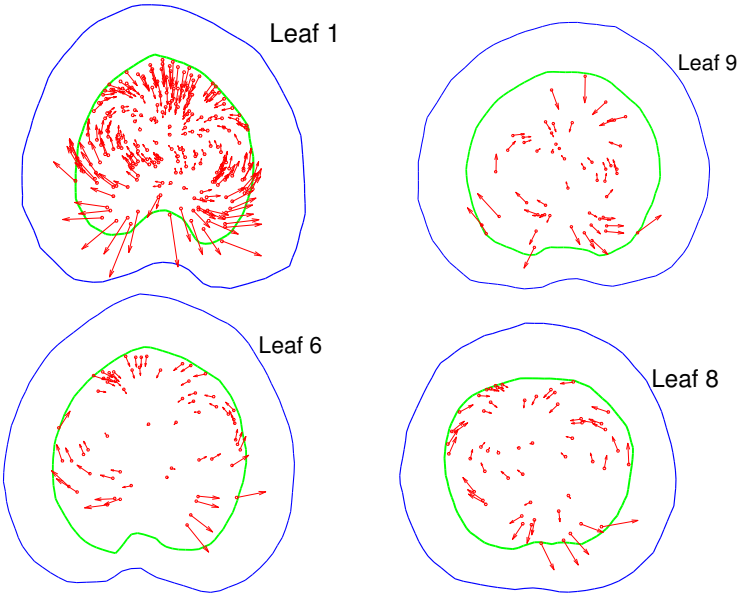

.

Figure 4: *Two complex functions, represented by arrows: the linear function,* $f(z) = 0.4z$ *and the quadratic one* $f(z) = 0.4iz^2$.

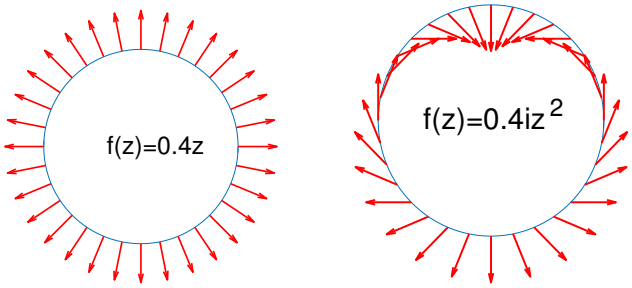

We therefore expect to get a better fit to the data with a quadratic complex polynomial $f(z) = a + bz + cz^2$, and this is indeed the case, as shown by the substantially smaller normalised quadratic residuals in Figure 2 and Table 3, with an average of 0.14, (86% of the displacement accounted for). Adding a cubic term, $f(z) = a + bz + cz^2 + dz^3$, gives a further small improvement, with 0.11 residual or 89% of the displacement accounted for; see Figure 2 and Table 3. Additional higher power terms give negligible improvement.

In addition to fitting a polynomial, one can also fit a Möbius transformation,

which has the form

$$f(z) = \frac{a + bz}{c + dz}.$$

Möbius transformations have the attractive property that the composition of two of them – i.e. following one by the other – is again a Möbius transformation. Furthermore, they have a matrix representation that is very useful for interpolating between the observations, as will be discussed later. It turns out that one gets almost as good a fit from a Möbius transformation as from a cubic, with an average residual of 0.12, or 88% of displacement accounted for; see Figure 2 and Table 3.

Figure 5: *The residual from the best fitting complex polynomial, for four leaves from days 7-8. The small circles representing beads have been removed so that the arrows can be seen more clearly.*

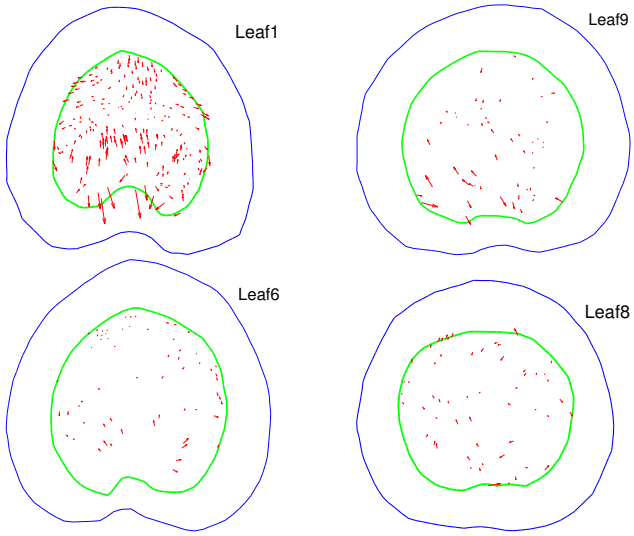

To summarise so far, a linear conformal map, which is equivalent to constant RGR, can account for about 67% of the displacement of beads, whereas a nonlinear conformal map, cubic or Möbius, accounts for 88-89% of the displacement (these are figures averaged over all leaves, for days 7 to 8). There is therefore a substantial nonlinear component to the conformal growth.

The residual of the best-fitting conformal map highlights regions of anisotropic or directional growth. As can be seen from Figure 5, there is considerable variation between individual leaves, some having marked anisotropic basal growth and others having very little. Basally localised anisotropic growth has previously been observed in averaged leaf data, e.g. Figure 7 in [2]. What is new here is the large amount of individual variability in this anistropic component.

Figure 6: *A: heat map of the relative growth due to the best-fitting conformal map for leaf 1, from days 7-8. The relative growth is calculated as* $\sqrt{\det J}$*, where* J *is the Jacobean of the best fitting complex map* $f(x, y)$ *and* det *its determinant. Using the Cauchy-Riemann equations (Eqs. 1, 2) this can be written as* $\sqrt{u_x^2 + u_y^2}$*, where* u *is the real part of the map* f*. B: The relative growth along the midvein.*

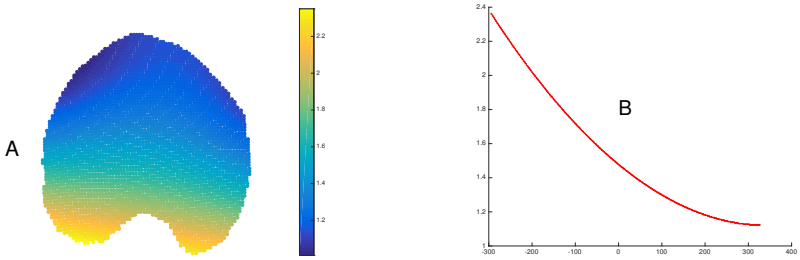

The leaves also show a strong basal bias in the *isotropic* growth rate. This can seen in the best-fitting conformal map; for instance Figure 6 shows that there is a strong gradient in the distribution of relative growth for leaf 1 from day 7 to 8. Unlike anisotropic growth, this pattern is found in all the leaves. This is well documented in the literature [7, 3], though fitting a conformal map clarifies the distinction between oriented and isotropic components in this gradient.

The data set allows one to follow the pattern of residuals for five successive time steps, beginning with 7-8 days. Figure 7 shows residuals averaged over all leaves: the linear residual gets steadily smaller, implying that the component of constant RGR increases steadily, so that some 85% of the growth is constant expansion by days 11-12. The pattern of linear residuals for an individual leaf (leaf 1) over five successive days is shown in Figure 8, and it tells the same story, with the initially large residuals at the apex and base of the leaf gradually diminishing.

Figure 7: *Change in the average residuals (linear and cubic) over time, showing the decrease in the linear residuals, and hence the increasingly large component of constant RGR, as the leaves age.*

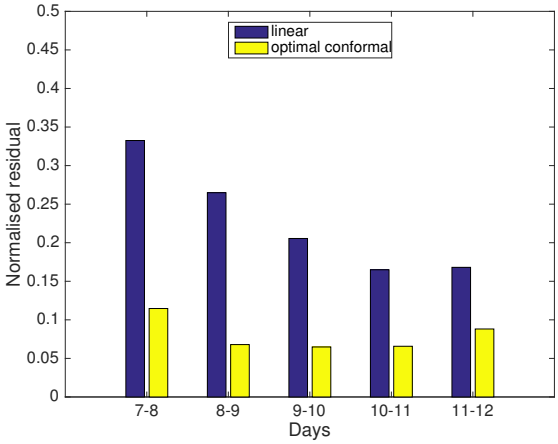

Figure 8: *The linear residual for leaf 1 from day 7 to day 12.*

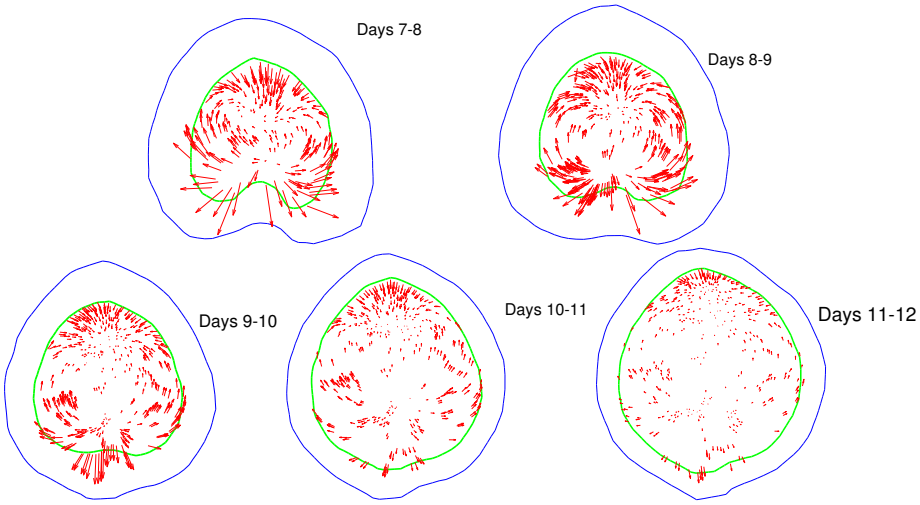

The biological meaning of conformal growth

A conformal map is a very special type of map, and it is natural to ask how it could be generated biologically. One might wonder whether it could be produced by requiring growth to be isotropic and at the same time ensuring flatness by some mechanical process, for instance by a comparison of stresses in the adaxial and abaxial surfaces coupled to a slowing of growth in areas where curvature develops. However, isotropic growth cannot be imposed locally, since it depends on

the growth and stresses in the surrounding tissue. It seems necessary therefore to have some global control, and Wolfram's proposal is that the concentration of a diffusing signal molecule could serve to specify the RGR of cells in the leaf [11].

It is not at all obvious that this mechanism will always yield a conformal map. However, suppose a conformal map results from growth over some time period. Then one can break this time period down into a sequence of short time steps (Eq. 5), in each of which growth produces only small displacements. These small displacements are also conformal, and in the limit of small intervals define the *infinitesimal generator* of the whole time sequence (Eq. 6). Like any conformal map, the infinitesimal generator is equivalent to a complex analytic function, and the RGR turns out to be the real part of the derivative of this function (Eq. 7). But the real part of any analytic function is always harmonic, i.e. it always obeys the equilibrium diffusion equation (Eq. 3). Conversely, given a signal molecule in diffusional equilibrium, this defines an infinitesimal generator which, on iteration, generates a conformal map for any time period.

If the growth map is a Möbius transformation, $f(z) = (a + bz)/(c + dz)$, one can represent the transformation by the matrix $A = \begin{pmatrix} b & a \\ d & c \end{pmatrix}$, and one finds that composing two Möbius transformations is equivalent to multiplying their matrices. Given an observed map over some time period (24 hours for the data used here), one can take a fractional power of the associated matrix and estimate the map for a shorter time period than the original 24 hours. Figure 9 illustrates the method by taking the square root of the matrix A for the best-fitting Möbius transformation for leaf 4 between days 7 and 8; the matrix $\sqrt{A}$ gives an estimate of growth in half the period of observation, i.e. 12 hours. One can take smaller fractional powers for shorter times, and in the limit this enables one to calculate the infinitesimal generator (Eqns 8, 9 and 10), and hence the distribution of the RGR everywhere on the leaf.

Figure 9: *Factorising the growth into two 12 hour periods, using the Möbius transformation with matrix $\sqrt{A}$, where A represents the best fit for the 24 hours between days 7 and 8 (leaf 4). The composition of the two maps, i.e. the result of following the red arrows and then the blue arrows, is equivalent to the 24 hour best fit.*

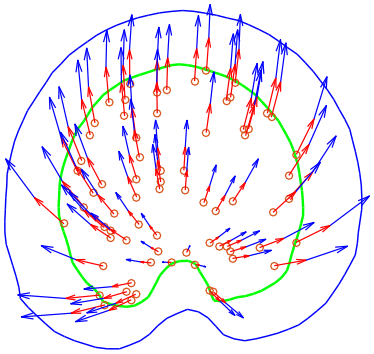

It turns out that the RGR is specified by a linear gradient of signal (Eq. 12). The constants that determine this gradient are given in Table 1 for leaf 1 over five successive day periods. There is a steady decrease in the average growth rate with time ($b_0 - c_0$), and also a decrease in the slope in the direction of the leaf axis (d_1), which accords with the decreasing nonlinear terms shown in Figures 7 and 8. If the source and sink concentrations at the margins remained fixed as the leaf elongated, this might account for a decrease in the slope, since the product of slope and length, Ld_1, gives the concentration difference. However, this product decreases over time (see Table 1), so this is not an adequate explanation (though, intriguingly, the product $L^2 d_1$, or area $\times$ slope, remains roughly constant throughout the five days).

Table 1: *The constants specifying the linear gradient in the RGR for leaf 1 over five successive day-lengths. The gradient is given by Eq. 12 as* $RGR(x, y) = (b_0 - c_0) - 2d_0 x - 2d_1 y$. *Growth is over 24 hours, so the units for* $b_0 - c_0$ *are per day, and for* d_0 *and* d_1 *are per millimetre per day. The last two columns show the length, L, of the leaf axis, in millimetres, and the product* Ld_1.

days	$b_0 - c_0$	d_0	d_1	L	Ld_1
7-8	0.4457	0.038	0.574	0.631	0.362
8-9	0.4362	0.015	0.271	0.944	0.256
9-10	0.3391	0.004	0.120	1.529	0.183
10-11	0.2686	-0.006	0.051	2.359	0.120
11-12	0.2099	0.003	0.026	3.018	0.078

Figure 10: *A: The linear gradient in RGR. Its minimum value is at the distal tip of the leaf, where growth is slowest, and its largest values at the base (compare with Figure 6). B: The gradual flattening of the gradient in RGR with successive days. Each line represents the gradient along the midvein. C: The flux pattern associated to a linear gradient set up by diffusion, and the distribution of sources (red) and sinks (green), calculated for the outline of leaf 1, that would be needed to generate the gradient.*

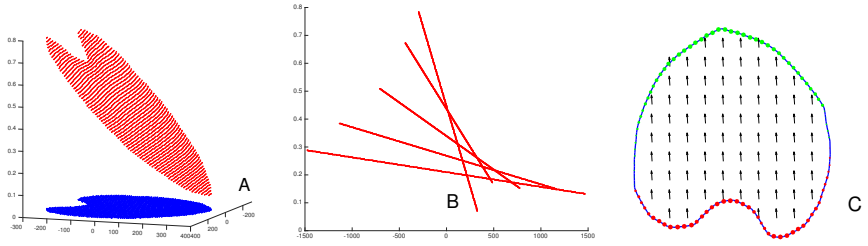

The idea of gradients of morphogens and read-out by measuring concentration is of course well-established [12], and linear gradients seem a natural option,

given that sources at one end of a segment and sinks at the other can readily generate them. However, in the case of Bicoid [13], for example, the gradient is exponential, and it is its log that is rather accurately linear [14]. And for the leaf, making a linear gradient by diffusion is not straightforward in the first place, since the outline of the leaf is irregular, and there needs to be a rather special layout of sources and sinks to ensure linearity (see Figure 10 C).

Thus the linear gradient of RGR does not necessarily mean that there is a linear gradient of a diffusing signal, with linear readout. However it is likely that diffusion is involved in setting up the distribution of the signal, whatever its shape. One should ask, therefore, whether a signal molecule could reach equilibrium over the entire leaf lamina, which might be of the order of 0.5 cm across at later stages of growth.

If we follow Crick's calculation [15], the time for diffusive equilibrium to be reached with 1% accuracy is given by $0.5L^2/D$ seconds, where L is the distance in cm and D is the diffusion constant in $\mathrm{cm}^2\mathrm{sec}^{-1}$. With L=0.5 cm and $D = 2.2 \times 10^{-6}$ $\mathrm{cm}^2\mathrm{sec}^{-1}$ (the cytoplasmic diffusion constant for auxin estimated in [16], and a larger value than Crick assumes), we find that the time is about 16 hours. Considering that Crick's calculation assumed de novo establishment of the gradient, whereas the gradient in the leaf starts from a previous equilibrium and only has to adjust to the increase in size, this time is probably a considerable overestimate, and a close approximation to equilibrium seems a reasonable assumption.

Discussion

The growth patterns of the leaves studied here have a significant nonlinear component (Figure 3), yet it turns out that they can be explained by a simple linear gradient of growth rate (Figure 10 A and B). This could arise from a linear gradient of a diffusible signal [11] and a linear read-out. It is an appealing idea that any source or sink arrangement on the margin of a leaf will create a signal distribution that is guaranteed to produce a conformal map and hence a flat leaf. One might then expect to find other shapes of signal distribution in other leaves. However, it could also be that nature only uses linear gradients of RGR, and that more elaborate leaf shapes are made by more elaborate developmental programs. If that is the case, the artificiality of making a linear diffusion gradient within the irregular form of a leaf (Figure 10 C) suggests that there might be some other underlying mechanism.

There is already a fairly detailed analysis of leaf growth in terms of developmental programs [1, 2, 3, 4, 5, 6, 7, 8], and it would be interesting to bring this into register with the conformal map viewpoint. Can the action of the factors PGRAD and LATE in the leaf shape model of Kuchen et al. [7] be explained by the linear growth rate in the conformal picture and its diminishing slope with time (Table 1 and Figure 10)? One difference is that PGRAD levels are assumed to be inherited by lineage and therefore to deform with the growth of the tissue [7], whereas the linear RGR in our conformal picture changes dynamically,

perhaps by diffusive equilibration. There is also no indication of a distinction between lamina and midvein growth (formalised by the factors LAM and MID [7]) in the residuals from the best-fitting conformal map (e.g. Figure 5). However, this may just be a matter of resolution, since the domain of operation of MID is quite narrow.

It would also be interesting to understand how the mechanism proposed to explain indentations in *Arabidopsis* leaves [17, 18] fits with a conformal viewpoint. Is this a developmental subroutine tacked onto the conformal growth plan of the lamina, or is it integrated into the underlying RGR distribution to make a harmonic map?

Materials and Methods

Data and analysis programs

The two papers from Prof. Rolland-Lagan's laboratory, [2, 3], give a thorough description of growth patterns and point the reader towards a website (http://hdl.handle.net/10393/30401) where the bead data for individual leaves are available, and also a package of Matlab programs for leaf shape analysis. Leaves are referred to by pot and plant numbers in their data sets, and Table 2 shows how this relates to the numbering used here.

Table 2: *The numbering of leaves used here (in order of decreasing number of beads), and the numbering in [2, 3], defined by the pot and plant. Also given is the number of beads on each leaf.*

My numbering	POT	PLANT	number of beads
1	19	1	231
2	19	2	82
3	1	2	80
4	3	3	71
5	7	1	68
6	3	2	62
7	3	1	57
8	7	2	55
9	5	1	51
10	20	1	36
11	17	1	32
12	1	1	26
13	7	3	22

Fitting conformal maps

Conformal maps are fitted by least squares. For instance, a quadratic map $f(z) = a + bz + cz^2$, with $z = x + iy$, can be written in the form $f(z) = u(x, y) + iv(x, y)$, where

$$u(x, y) = a_0 + b_0 x - b_1 y + c_0(x^2 - y^2) - 2c_1 xy,$$

and

$$v(x, y) = a_1 + b_0 y + b_1 x + c_1(x^2 - y^2) + 2c_0 xy,$$

with $a = a_0 + ia_1$, $b = b_0 + ib_1$, $c = c_0 + ic_1$. If the coordinates of bead k at time 1 are $(x_1^{(k)}, y_1^{(k)})$ and at time 2 are $(x_2^{(k)}, y_2^{(k)})$, then we find the values of $a_0, a_1, b_0, b_1, c_0, c_1$ that minimise the sum S given by

$$S = \sum_k \left(u(x_1^{(k)}, y_1^{(k)}) - x_2^{(k)} \right)^2 + \left(v(x_1^{(k)}, y_1^{(k)}) - y_2^{(k)} \right)^2 .$$

The minimisation is a linear problem that can be done very rapidly by linear algebra functions in Matlab.

The Möbius transformation is fitted by writing the function $f(z) = (a + bz)/(c + dz)$ as a polynomial series, viz. $f(z) = (a/c + b/c)(1 - dz/c + d^2 z^2/c^2 - \ldots)$, and comparing its terms up to quadratic order with those of the best-fitting cubic. This determines a, b, c, d, up to an irrelevant shared factor. The cubic term in the expansion is then found to be quite closely approximated by that of the best-fitting cubic (which is in any case a very small term). In other words, the best-fitting cubic is already quite close to a Möbius transformation. This can be seen in the small changes in the residuals in Table 3.

Table 3: *Normalised residuals after least-squares fitting to either linear or third-degree conformal maps. The normalised residual is defined as* $\sum_i |v_i - l_i| / \sum_i |v_i|$*, where* $|v_i|$ *is the length of the vector* v_i *between bead positions on successive days,* l_i *is the vector, and* i *runs over all beads.*

Leaf	linear residual	quadratic residual	cubic residual	Möbius residual
1	0.289	0.124	0.101	0.103
2	0.449	0.202	0.141	0.148
3	0.381	0.158	0.135	0.130
4	0.376	0.164	0.138	0.141
5	0.406	0.209	0.165	0.178
6	0.247	0.083	0.052	0.065
7	0.325	0.117	0.110	0.112
8	0.348	0.145	0.092	0.116
9	0.301	0.121	0.099	0.107
10	0.261	0.123	0.097	0.118
11	0.360	0.178	0.180	0.193
12	0.253	0.101	0.101	0.105
13	0.327	0.104	0.080	0.088
average	0.333	0.141	0.115	0.123

Analytic functions and diffusion

Let f be a complex analytic function. This means that f is differentiable as a complex function (as are all the functions one is likely to encounter in the present context). We can write the function in terms of its real and imaginary parts as $f(x, y) = u(x, y) + iv(x, y)$, where $x + iy$ is the point with coordinates x, y in the complex plane. Calculating the derivative of f by a real δx gives $f' = u_x + iv_x$ (where u_x denotes $\partial u/\partial x$, etc.), whereas making the calculating with an imaginary $i\delta y$ gives $f' = -iu_y + v_y$. Equating these two definitions yields the Cauchy-Riemann equations,

$$u_x = v_y, \tag{1}$$
$$u_y = -v_x. \tag{2}$$

These in turn imply that

$$u_{xx} + u_{yy} = 0, \tag{3}$$
$$v_{xx} + v_{yy} = 0, \tag{4}$$

(where $u_{xx} = \partial^2 u/\partial x^2$, etc.), implying that both u and v satisfy Laplace's equation, which is the equation for the equilibrium distribution of a diffusing substance [19]. A function satisfying this equation is called a *harmonic* function.

Thus both the real and imaginary parts of f are harmonic. Conversely, given a harmonic function u, the Cauchy-Riemann equations can always be solved to give v, and this yields a conformal map with real and imaginary parts u and v.

The relative growth rate of a conformal map family

We begin with an assumption, that is only an approximation to biological reality, that growth results from the repeated iteration of the same map that operates over a short time period. Thus we define the map $f_{1/n}$ to be the map whose n-fold composition is the map $f(z)$ observed over some time interval (e.g. the 24 hours of the observations here). In other words

$$f(z) = f_{1/n}(f_{1/n}(\dots f_{1/n}(z)\dots)). \tag{5}$$

We assume that such a map $f_{1/n}$ exists for arbitrarily large n (i.e. arbitrarily short times). The reason this is not biologically fully plausible is that the map is likely to change as the leaf grows: what we are calling $f_{1/n}$ will not be quite the same map at the beginning and end of a sequence of iterations. However, the simplifying assumption makes the problem mathematically tractable, and is enshrined in the concept of a semigroup of maps, where $f_{s+t}(z) = f_s(f_t(z))$, for all positive s, t [20].

For large n, the map $f_{1/n}(z)$ is close to the identity, and can therefore be written approximately as

$$f_{1/n}(z) \approx z + \frac{g(z)}{n}, \tag{6}$$

where $g(z)$ is called the *infinitesimal generator* of the semigroup [20]. If $f(z)$ is conformal, so is $f_{1/n}(z)$ and so is the infinitesimal generator. Now define the relative growth $RG_f(z)$ for the map $f(z)$ at the point z as $|f'(z)|$. The relative growth *rate*, $RGR(z)$, which is what we want to find, is the temporal derivative of $RG(z)$. If $g(z)$ has real and imaginary parts h and k, respectively

$$\begin{aligned} RGR_f(z) &= \lim_{n\to\infty} \frac{RG_{f_{1/n}}(z) - z}{1/n}, \\ &= \lim_{n\to\infty} n(|1 + g'(z)/n| - 1), \\ &= \lim_{n\to\infty} n\left[\sqrt{(1 + h_x/n)^2 + h_y^2/n^2} - 1\right], \\ &= h_x. \end{aligned} \tag{7}$$

Now h_x, which is the real part of the analytic function $g'(z)$, is harmonic. So the growth rate could be specified by the concentration of a substance at diffusive equilibrium. These steps can be reversed, since any harmonic function can be written as the real part of some complex function $k(z)$ and we can take the conformal infinitesimal generator to be $g(z) = \int k(z)$. Since composition of conformal maps is conformal, the resulting growth is conformal. So specifying the growth rate by the concentration of a diffusible substance produces a conformal map, a conclusion reached by a different argument, far more tersely and elliptically, in [11].

The relative growth rate of a Möbius transformation family

Calculating the infinitesimal generator is easy for a Möbius transformation f. If A is the matrix representing f, then $A^{1/n}$ is the matrix representing $f_{1/n}$ (see Figure 9 for an illustration of $f_{1/2}$). In the limit of large n,

$$A^{1/n} \approx \mathrm{id} + \frac{\log A}{n}, \tag{8}$$

where $\log A$ is the matrix logarithm of A. Writing

$$\log A = \begin{pmatrix} b & a \\ d & c \end{pmatrix}, \tag{9}$$

and converting the matrix $A^{1/n}$ back into a Möbius transformation gives (neglecting terms in $(1/n)^2$ or higher powers)

$$\begin{aligned} f_{1/n}(z) &\approx [a/n + (1 + b/n)z]\,[1 - c/n]\,[(1 + c/n) - (d/n)z] \\ &\approx z + g(z)/n, \end{aligned} \tag{10}$$

where

$$g(z) = a + (b - c)z - dz^2 \tag{11}$$

Thus the infinitesimal generator $g(z)$ is a quadratic polynomial. Eq. 7 now gives

$$RGR_f(z) = h_x(z) = \Re g'(z) = \Re\{(b - c) - 2dz\} = (b_0 - c_0) - 2d_0x - 2d_1y, \tag{12}$$

where b, c, d are the entries in $\log(A)$ defined above with $b = b_0 + ib_1$, $c = c_0 + ic_1$, $d = d_0 + id_1$. Thus three real parameters are needed to define the growth.

Acknowledgements

I thank Anne-Gaëlle Rolland-Lagan for allowing me to use her data, Benoit Tremblay for help with the Matlab package that allows one to manipulate the data, Konrad Wagstyl for an introduction to Matlab programming, and Julie Ahringer and Ottoline Leyser for helpful critical comments.

References

[1] Rolland-Lagan A-G, Bangham JA, Coen E. 2003. Growth dynamics underlying petal shape and asymmetry. Nature 422, 161-3. doi:10.1038/nature01443.

[2] Remmler L, Rolland-Lagan A-G. 2012. Computational method for quantifying growth patterns at the adaxial leaf surface in three dimensions. Plant Physiol. 159:27-39. doi: 10.1104/pp.112.194662.

[3] Rolland-Lagan A-G, Remmler L, Girard-Bock C. 2014. Quantifying shape changes and tissue deformation in leaf development. Plant Physiol. 165:496-505. doi.org/10.1104/pp.113.231258

[4] Cui M-L, Copsey L, Green AA, Bangham JA, Coen E. 2010. Quantitative control of organ shape by combinatorial gene activity. PLoS Biology 8(11) e1000538. doi:10.1371/journal.pbio.1000538.

[5] Green AA, Kennaway JR, Hanna AI, Bangham JA, Coen E. 2010. Genetic control of organ shape and tissue polarity. PLoS Biology 8(11) 1000537. doi:10.1371/journal.pbio.1000537.

[6] Kennaway R, Coen E, Green A, Bangham JA. 2011. Generation of diverse biological forms through combinatorial interactions between tissue polarity and growth. PLoS Comput Biol 7(6): e1002071. doi:10.1371/journal.pcbi.1002071.

[7] Kuchen EE, Fox S, Barbier de Reuille P, Kennaway R, Bensmihen S, Avondo J, Calder GM, Southam R, Robinson S, Bangham A, Coen E. 2012. Generation of leaf shape through early patterns of growth and tissue polarity. Science 335:1092-6. doi: 10.1126/science.1214678. doi.org/10.1126/science.1214678

[8] Sauret-Güeto S, Schiessl K, Bangham A, Sablowski R, Coen E. 2013. JAGGED controls *Arabidopsis* petal growth and shape by interacting with a divergent polarity field. PLOS Biology 11, e1001550. doi:10.1371/journal.pbio.1001550.

[9] Thompson D'A W. 1917. On growth and Form. Footnote p 1084. Cambridge University Press 1968.

[10] Jones GW, Mahadevan L. 2013. Planar morphometry, shear and optimal quasi-conformal mappings. Proc. R Soc. A 469:20120653. doi: 10.1098/rspa.2012.0653

[11] Wolfram S. 2002. A new kind of science. Note on 'Locally isotropic growth', p 1007. Wolfram Media Inc.

[12] Wolpert L. 1969. Positional information and the spatial pattern of cellular differentiation. J. Theor. Biol. 25 (1): 147. doi:10.1016/S0022-5193(69)80016-0.

[13] Driever W, Nsslein-Volhard C. 1988. The bicoid protein determines position in the Drosophila embryo in a concentration-dependent manner. Cell 54: 95–104. doi: 10.1016/0092-8674(88)90183-3

[14] Gregor T, Tank DW, Wieschaus EF, Bialek W. 2007. Probing the limits to positional information. Cell 130: 153–164. doi: 10.1016/j.cell.2007.05.025

[15] Crick F. 1970. Diffusion in embryogenesis. Nature 225, 420-422. doi: 10.1038/225420a0

[16] Rutschow HL, Baskin TI, Kramer EM. 2011. Regulation of solute flux through plasmodesmata in the root meristem. Plant Physiol. 155(4):1817-26. http://dx.doi.org/10.1104/pp.110.168187

[17] Bilsborough GD, Runions A, Barkoulas M, Jenkins H, Hasson A, Galinha C, Laufs P, Hay A, Prusinkiewicz P, Tsiantis M. 2011. Model for the regulation of *Arabidopsis thaliana* leaf margin development. Proc. Nat. Acad. Sci. USA, 108 (8) 3424-9. doi: 10.1073/pnas.1015162108.

[18] Engelhorn J, Reimer JJ, Leuz I, Göbel U, Huettel B, Farrona S, Turck F. 2012 DEVELOPMENT-RELATED PcG TARGET IN THE APEX 4 controls leaf margin architecture in *Arabidopsis thaliana*. Development 139, 2566-2575. doi:10.1242/dev.078618.

[19] Crank J. 1975. The mathematics of diffusion. Oxford: The Clarendon Press.

[20] Bracci F, Contreras MD, Diaz-Madrigal S. 2007. Infinitesimal generators associated with semigroups of linear fractional maps. Journal d'Analyse Math. 102, 119-142. doi 10.1007/s11854-007-0018-9.